SUPPLEMENTARY INFORMATION

Evidence of High Electron Mobility in Magnetic Kagome Topological Metal FeSn Thin Films

Lorenzo Mosesso[1*], Luca Tomarchio[1,2], Niraj Bhattarai[3], Salvatore Macis[1,4], Paola Gori[5], Antonio Grilli[4], Mariangela Cestelli Guidi[4], John Philip[3], Olivia Pulci[6] and Stefano Lupi[1,7]

[1]Department of Physics, Sapienza University, Piazzale Aldo Moro 5, 00185, Rome, Italy.
[2]INFN section of Rome, P.Le Aldo Moro, 2, 00185 Rome, Italy.
[3]Department of Physics and The Vitreous State Laboratory The Catholic University of America, Washington, DC 20064.
[4]INFN – Laboratori Nazionali di Frascati, via Enrico Fermi 54, 00044, Frascati (Rome), Italy.
[5]Department of Industrial, Electronic and Mechanical Engineering, Roma Tre University, Via della Vasca Navale 79, I-00146 Rome Italy
[6]Department of Physics, and INFN, University of Rome Tor Vergata, Via della Ricerca Scientifica 1, I-00133 Rome, Italy
[7]CNR–IOM, Area Science Park, Basovizza, Ed. MM, Strada Statale 14 Km 163,5, Trieste, I-34149, Italy

I. FeSn 80 nm

The optical spectroscopy investigation performed on the FeSn 20nm thin film has been carried out also for the 80 nm sample. Similar results to the ones proposed in the main text have been obtained, so analogous considerations will be proposed below. Figure S1a shows the real part of the optical conductivity at different temperatures from 20 K across the Neel temperature up to 400 K in a wide spectral range from THz (30 cm^{-1}) to Visible (25000 cm^{-1}). The linear optical response of the system is obtained from the simultaneous fitting procedure performed on the experimental reflectance and transmittance data as described in the Method section of the main text. The resulting temperature dependence of $\sigma_1(\omega)$ is almost identical to the one proposed for the 20 nm thin film in Fig.2a. At low energies, the Drude contribution associated to the electronic transport strongly emerges upon cooling due to the gradual redshift of

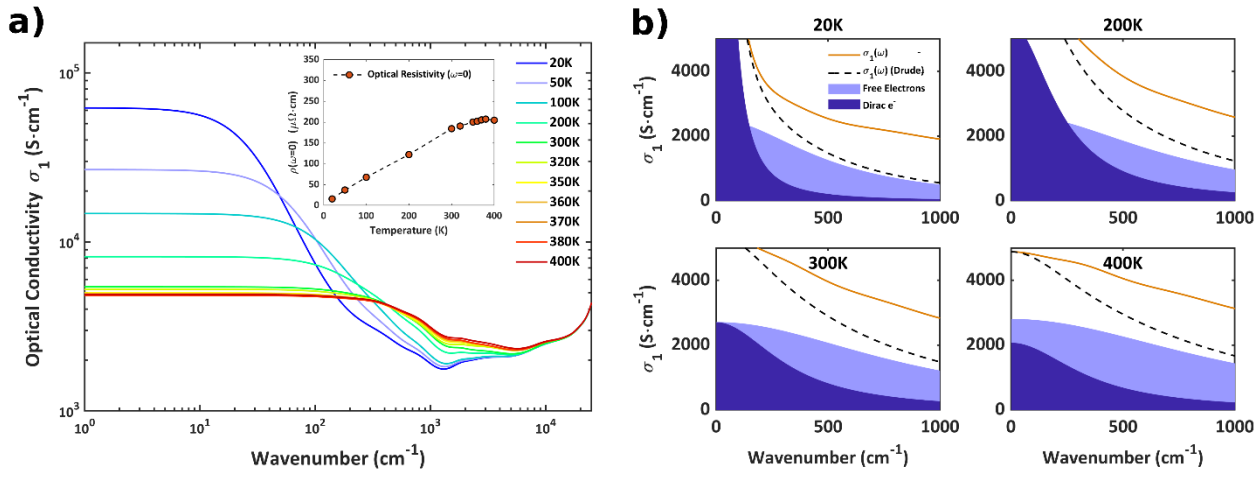

Figure S1| Temperature dependence of the optical conductivity for the FeSn 80 nm thin film: **a)** Real part of the optical conductivity $\sigma_1(\omega)$ at different temperatures. Above $\sim 320\ K$ the temperature dependence is almost constant, providing very small variations over the entire spectrum. The inset shows resistivity data extrapolated from $\sigma_1(\omega)$ and calculated at $\omega = 0$ (the dot dashed line is a guide for the eyes). **b)** Behaviour of the two Drude peaks (see main text) for four representative temperatures: 20, 200, 300 and 400 K. The Drude peak associated with massive free electrons (lighter blue) is weakly temperature-dependent. The Drude peak associated with Dirac electrons (darker blue), by contrast, broadens very rapidly with increasing temperature in conjunction with a progressive decrease in its amplitude. The red solid line corresponds to the full $\sigma_1(\omega)$ data while the black dashed lines include only the full Drude contribution to the conductivity

the metallic spectral weight, providing very high DC conductivity values below 300 K. The inset of Fig.S1a shows the zero-frequency optical resistivity defined as the inverse of the optical conductivity $\sigma_1(\omega)$ calculated at the frequency ω=0 as a function of temperature. The result is in agreement with DC resistivity measurements performed on 80 nm FeSn thin films deposited on Al_2O_3 [1].

The temperature dependence of the FeSn 80nm low-energy electrodynamics can be explained once again by means of the two-carrier model, that requires the exploitation of two Drude terms in the Drude-Lorentz model to correctly describe the multiband dynamics within the system (see main text).

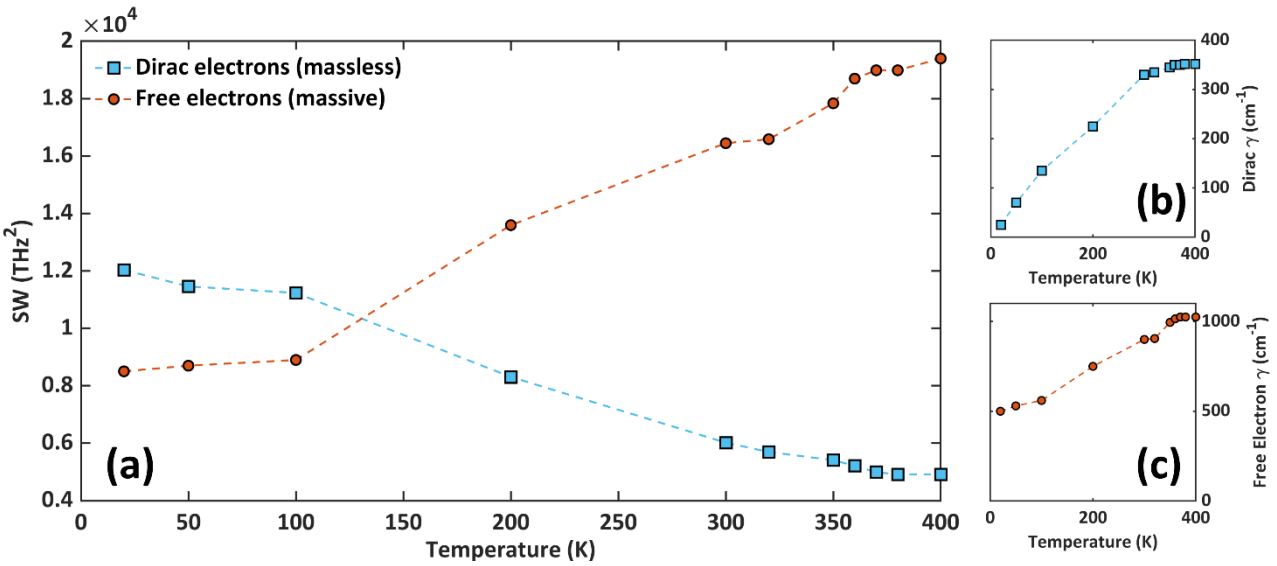

Figure S2| Spectral Weight SW and Scattering rate γ for the FeSn 80nm thin film: **a)** Temperature dependence of the Drude Spectral Weight for the two transport channels (see main text). Brown circles describe massive free electrons while blue squares are associated with Dirac electrons. **b,c)** Temperature dependence of the scattering rate calculated for both Dirac and massive electrons.

The temperature variation of the two Drude contribution is shown in Fig.S1(b) for four representative temperatures, namely 20, 200, 300 and 400 K. Here the lighter blue peak has slight variation with temperature, that corresponds to the small relative increase of both the plasma frequency ω_p and the scattering rate γ for increasing T (see also Fig.S2(a,c)). At variance, the darker blue Drude term changes strongly upon cooling due to the strong reduction of γ (Fig. S3(b)), that reaches the very low value of $20\ cm^{-1}$ at 20 K. This behaviour is analogous to what has been found for the 20nm thin film, so that the same association can be provided for the two Drude terms. The former (lighter blue) is associated to massive electrons populating the parabolic dispersive bands, while the latter (darker blue) is associated to the high mobility electrons populating the linear dispersive Dirac states characterizing the band structure of FeSn, as reported in the main text.

Fig. S2 shows the Drude Spectral Weight as a function of temperature calculated for the FeSn 80 nm sample, providing analogous results as the one reported in the main text (Fig. 3a) for the 20nm thin film. Here it is possible to notice the same spectral weight transfer between the two electron transport channels upon warming up, with the only difference that now the Dirac electron contribution exhibits a non-negligible weight even at the highest measured temperatures. The two electron transport channels show an almost constant SW below $100K$, indicating that the strong change in conductivity at low temperature is completely dominated by a change in the mobility of the Dirac electrons, which can be ascribed to an increasing scattering rate with temperature associated to the strong e-ph interaction characterizing the FeSn kagome metal [2]. Above $\sim 100\ K$ instead, the Drude contribution associated to the Dirac massless electrodynamics reduces its SW consistently due to concurrent phonon-induced inter-band scattering processes, which contribute to the homogenization of the transport into a single metallic transport channel. However, even well above room temperature, the 80nm thin film exhibits two distinct electronic transport channels characterized by distinct mobilities, at variance to what happens to the 20nm thin film in which the Dirac contribution becomes almost irrelevant already at 300K.

Above room temperature, the low-energy electrodynamics of the system exhibits small variations as temperature increases, together with a roughly constant behaviour of the inter-band contribution to the real part of the optical conductivity, showing a similar behaviour to the one proposed in the main text for the 20nm thin film. The optical response of the system over the entire spectrum therefore becomes nearly constant as the temperature changes, even across the magnetic transition at T=365K, indicating the preservation of the JDOS in spite of the fact that the magnetic ordering and corresponding symmetries can considerably affect the electronic transitions and the band structure in the system [3,4]. Fig.S3 shows the decomposition of the real part of the optical conductivity in the set of oscillators used for the construction of the Drude-Lorentz model for the FeSn 80nm thin film at 300K. The set of inter-band contributions is explained extensively in the main text, where the lack of kagome metal fingerprints characterizing low-energy electronic transitions is also highlighted. It is important to note that this decomposition changes slightly as a function of the thickness. By increasing the film thickness from 20 to 80nm, the inter-band contributions varies in the high energy range above $6000\ cm^{-1}$ (Fig.4 of the main text and inset of Fig.S3) and in the low-energy spectral range around $\sim 500\ cm^{-1}$, where the bulk realization is identified by the enhancement of the two oscillators centred at the resonance frequencies $\omega_0 \sim 390$ and $\omega_0 \sim 800 cm^{-1}$, which define the set of low-energy electronic transitions along the $\Gamma \rightarrow K$ direction.

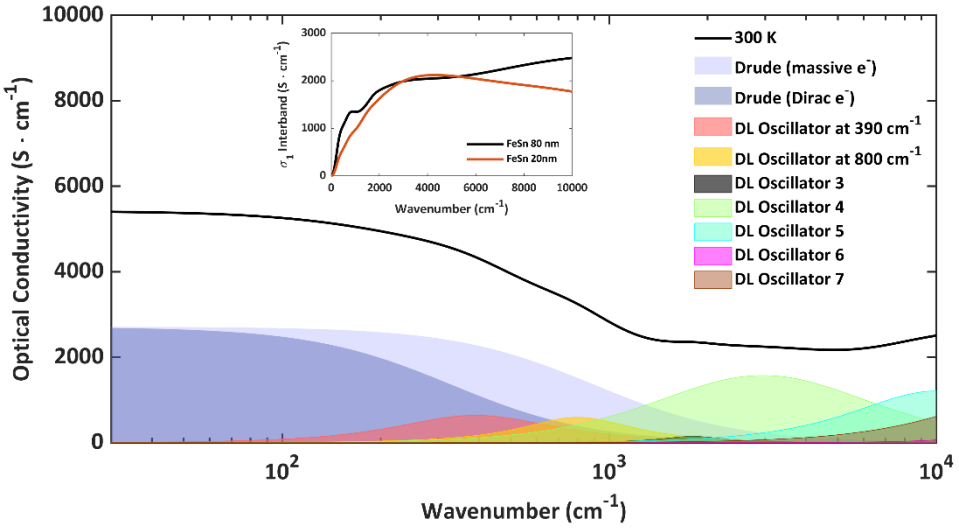

Figure S3| Decomposition of $\sigma_1(\omega)$ in its Drude-Lorentz oscillator: Drude-Lorentz model obtained by fitting the experimental optical data and implemented by superimposing two Drude contributions (one associated with Dirac electrons and one associated to massive electrons populating parabolic-like bands) together with few other Drude-Lorentz oscillators associated to inter-band electronic transitions. In the inset the inter-band contribution to the real part of the optical conductivity is reported for the 20 nm (red line) and the 80 nm (black line) thin films. This contribution has been obtained subtracting the Drude terms from $\sigma_1(\omega)$.

II. Theoretical electronic band structure

The DFT electronic band structure of bulk FeSn is reported in Fig. S4. The projection of the wavefunctions on the atomic orbitals allows to attribute the electronic states to Sn (blue circles), Fe (red circles) or to a hybridized Fe-Sn state (green circles). A state has been attributed to an atomic species if the projection is larger than 70%.
The Dirac cone appears at K, ~ 0.4 eV below the Fermi level, and derives from Fe states.

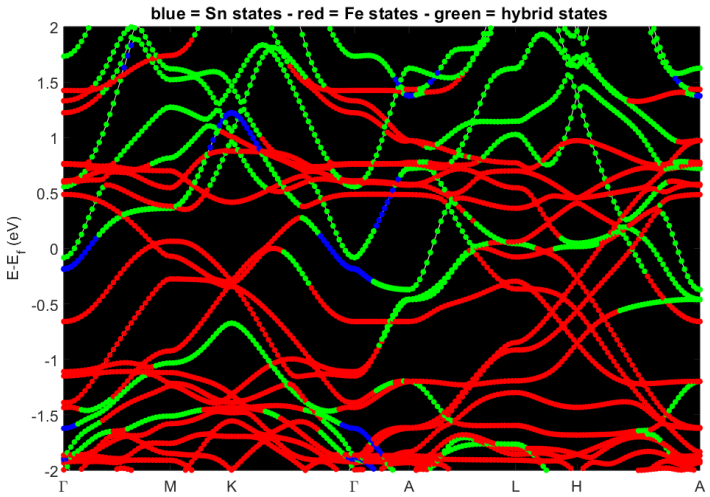

Figure S4| DFT electronic band structure of bulk FeSn. Red circles refer to Fe states, blue to Sn and green to hybrid states.

References

[1] D. Khadka, T. R. Thapaliya, J. Wen, R. F. Need, and S. X. Huang, High quality epitaxial thin films and exchange bias of antiferromagnetic Dirac semimetal FeSn.
Appl. Phys. Lett. 117, 032403 (2020)

[2] Sales, B. C., Saparov, B., McGuire, M. A., Singh, D. J. & Parker, D. S. Ferromagnetism of Fe3Sn and Alloys. Sci Rep 4, 7024 (2014).

[3] Kang, M. et al. Dirac fermions and flat bands in the ideal kagome metal FeSn. Nat. Mater. 19, 163–169 (2020), *Supplementary Materials*

[4] Ebad-Allah, J. et al. Optical anisotropy of the kagome magnet FeSn: Dominant role of excitations between kagome and Sn layers. Phys. Rev. B 109, L201106 (2024), *Supplementary Materials*